Proceedings of the 14th International Heat Transfer Conference
IHTC14
August 8-13, 2010, Washington, DC, USA

IHTC14-23202

HEAT TRANSFER DURING DROP IMPACT ONTO A HEATED SOLID SURFACE

A. S. Moita
Center for Innovation, Technology and Policy Research, IN+
Instituto Superior Técnico
Lisbon, Portugal

A. L. N. Moreira
Center for Innovation, Technology and Policy Research, IN+
Instituto Superior Técnico
Lisbon, Portugal

Ilia V. Roisman
Institute of Fluid Mechanics and Aerodynamics,
Center of Smart Interfaces
Technische Universität Darmstadt
Darmstadt, Germany

ABSTRACT

The present paper addresses the theoretical and experimental study of a liquid drop impacting onto a solid heated substrate. The experiments encompass the measurement and evaluation of the instantaneous substrate and contact temperatures, for different impact conditions and various thermodynamic properties of the liquid and target. Initial surface temperatures are varied from the ambient temperature up to slightly above the boiling temperature of the liquids (T_{W0max}=120ºC), for different surface materials, covering significantly different wall effusivities, thus allowing to validate the model for extreme conditions. The theory is based on the remote self-similar analytical solution of the Navier-Stokes equations in the spreading drop coupled with the energy equation, which allows obtaining a theoretical solution for the flow field and temperature field in the liquid region. An explicit analytical expression is proposed for the contact temperature, which is expressed, not only through the thermal effusivities of the solid and liquid materials and their initial temperature, but also depends on the Prandtl number. The theory predicts a constant value of the contact temperature in the phase when the thermal boundary layer is thinner than the thickness of the lamella.

The model is validated by comparison with the experimental data. The agreement is rather good despite the fact that no adjustable parameters are introduced in the model.

INTRODUCTION

The investigation of the fluid dynamic and heat transfer phenomena occurring at the liquid-solid interface of drops impacting onto heated substrates is motivated by a wide range of industrial applications, many of them related to cooling systems, e.g. for metallurgy (1,2), ink jet printing (3), cooling of electronic parts (4) or in medical applications (5).

When a drop impacts onto a solid surface it deforms and spreads on its surface creating a radially expanding thin lamella bounded by a rim. If the temperatures of the drop and of the substrate are different, the temperature at the interface (the contact temperature) is determined by heat conduction within the substrate and by convection with the spreading drop. The value of the contact temperature determines the rate of heat exchange between the drop and the target. However, the transport processes involved during drop/surface contact are not completely understood yet. This is the objective of the present study, where the impact of a liquid drop onto a solid heated surface is investigated experimentally and modelled theoretically.

Studies reporting measurements of the instantaneous substrate and contact temperatures are quite scarce in the literature. A constant and uniform surface temperature was early suggested by Seki et al. (6), who assumed that the temperature at the liquid-solid interface is given by the contact temperature obtained from the solution of the heat transfer equation for two semi-infinite solids: $T_c=[(T_w.\ \varepsilon_w+T_l.\varepsilon_l)/(\ \varepsilon_w+\varepsilon_l)]$, where ε_w and ε_l are the thermal effusivities of the substrate and of the liquid, respectively, $\varepsilon=(\rho k C_p)^{1/2}$, ρ is the specific mass, k is the thermal conductivity and C_p is the specific heat. More recent work report measurements of the substrate temperature for sessile drops, e.g. by Abu-Zaid and Atreya (7) and by Tartarini et al. (8,9). The variation of the surface temperature during drop impact was measured by Labeish (10), Chen and Hsu (11) and Pasandideh-Fard et al. (12).

The experimental part of the work considers the study of the boiling morphology and the measurement of the temperature at the contact region of the liquid drop with the heated substrate. The contact temperature is evaluated for

different impact conditions, covering a wide range of dissimilar liquid and surface effusivities.

Theoretical models of liquid vaporization and prediction of liquid and surface temperatures were also proposed by few authors, such as di Marzo and Evans (13,14), di Marzo et al. (15,16) and Chandra et al. (17). These models were developed for sessile drops, considering a constant and uniform liquid-solid interface temperature (exception made to di Marzo et al., [16] who solved the transient conduction equations numerically for the liquid and solid phases). Pasandideh-Fard et al. (12) and Healy et al. (18) provide numerical predictions of the liquid and substrate temperatures and of the heat flux, for impacting drops.

In the model proposed here, the substrate is considered as a semi-infinite body with constant thermodynamic properties. Just after collision, two thermal boundary layers develop, one on the side of the substrate and the second on the side of the spreading drop. The thicknesses of both boundary layers increase with the square root of time. The thickness of the thermal boundary layer on the liquid side is influenced by the heat transfer and by the liquid flow. The theory is based on the remote self-similar analytical solution of the Navier Stokes equations in the spreading drop, which allows obtaining a similarity solution for the temperature field in the liquid region. The condition of the continuity of the temperature and continuity of the heat flux at the drop/substrate interface allows to determine an explicit analytical expression for the contact temperature, which is expressed, not only through the thermal effusivities of the solid and liquid materials and their initial temperature, but also through an explicit dependence on the Prandtl number.

The model is validated by comparison with the experimental data.

NOMENCLATURE

C_p	Specific heat [$kJkg^{-1}K^{-1}$];
D	Drop diameter [mm];
k	Thermal conductivity [$Wm^{-1}K^{-1}$];
Pr	Prandtl number ($=C_p\mu/k$);
r	Radial coordinate [mm];
Re	Reynolds number ($=\rho u_0 D_0/\mu$);
T	Temperature [ºC];
t	Time [s];
t*	Dimensionless time ($=t/(D_0/u_0)$);
u	Velocity component normal to the surface [ms^{-1}];
We	Weber number ($=\rho D_0 u_0^2/\sigma_{lv}$);
z	Axial coordinate [mm].

Greek Symbols

ΔT	Temperature difference [ºC];
α	Impact angle [º];
ν	Kinematic viscosity [m^2s^{-1}];
θ	Static contact angle [º];
σ_{lv}	Surface tension of the liquid [Nm^{-1}];
μ	Dynamic viscosity [$kgm^{-1}s^{-1}$];
ρ	Specific mass [kgm^{-3}];
ξ	Self-similar coordinate;
ε	Thermal effusivity ($=\rho k C_p^{1/2}$) [$W^{-1}s^{1/2}/m^2K$].

Subscripts

0	Initial (t=0s);
c	Contact;
CHF	Critical Heat Flux;
d	Drop;
max	Maximum;
sat	Saturation;
w	Wall.

EXPERIMENTAL METHOD

The experiments reported here encompass the normal impact (i.e. with a fixed impaction angle of α=90º) of individual drops of different liquids, namely water, ethanol and methoxy-nonafluorobutane - $C_4F_9OCH_3$ (HFE7100) - onto heated targets. The impact conditions are varied to cover a broad range of the most relevant dimensionless groups, (65 < Weber number, We < 1314; 170 < Reynolds number, Re < 11140). The working conditions are summarized in Table 1, while Table 2 depicts the thermo-physical properties of the liquids.

Table 1: Experimental conditions.

Liquid	Parameters		
	D_0 [mm]	u_0 [ms^{-1}]	T_{w0} [ºC]
Water	$2.8 \le D_0 \le 3.0$	$0.4 \le U_0 \le 3.1$	Room temp. $\le T_W < 120$
Ethanol	$2.2 \le D_0 \le 2.4$	$0.4 \le U_0 \le 2.5$	Room temp. $\le T_W \le 120$
HFE7100	$1.7 \le D_0 \le 2.0$	$0.4 \le U_0 \le 2.5$	Room temp. $\le T_W \le 115$

Table 2: Thermo-physical properties of the working fluids.

Working Fluids	Water	Ethanol	HFE7100
Surface Tension [Nm^{-1}]x10^3	73.75	22.0	13.6
Specific mass [kgm^{-3}]	998	790	1430
Kinematic viscosity [m^2s^{-1}]x10^6	1.0	1.4	0.38
Specific heat [$kJkg^{-1}K^{-1}$] (20ºC)	4.18	2.44	1.18
Thermal conductivity [$Wm^{-1}K^{-1}$]x10^3	606	169	68.8
$T_{sat.}$ [ºC]	100	78.3	61.0

These are the reference values taken at 25ºC and their variation with the temperature is considered as in Turns (19), Ozisik (20), Incropera and DeWitt (21), Lemmon et al. (22), and in the 3M Database for the HFE7100.

As shown in Table 1, the initial surface temperature, T_{w0} varies from the ambient temperature up to slightly above the boiling temperature of the liquids (T_{w0max} = 120ºC), to avoid liquid phase change within the spreading lamella.

The substrates are accommodated on a copper base inside which a 264 W cartridge heater is inserted.

The surface temperature of the targets is monitored by thermocouples type K and controlled by a PMA KS20-I temperature controller. One of the thermocouples is a fast response "Medtherm" eroding-K-type which is embedded at the centre of the region where droplets impact. The signal of the thermocouples is sampled with a National Instruments DAQ board plus a BNC2120 and amplified with a gain of 300 before processing. Morphology of drop impact is characterized with two synchronized high-speed cameras, as in Moita and Moreira (23, 24). The former, which provides side view images of the spreading lamella, is a Kodak Motion Corder Analyser, Series SR 512x420pixels, Model PS-120, with a maximum frame rate of 10kfps. The second allows visualizing the liquid-solid interface from the back of the surface and is a Phantom v4.2 from Vision Research Inc., with 512x512pixels@2100fps and a maximum frame rate of 90kfps. Visualization of the liquid-solid interface is possible making use of a transparent smooth glass surfaces heated by Joule effect from the back side with a transparent film of Indium Oxide, In_2O_3. Deposition of the film is made by radio frequency (rf) plasma enhanced reactive thermal evaporation (rf-PERTE) at low substrate temperature (<100ºC). Details of the method and of the resulting relevant film properties are reported by Carvalho et al. (25). A similar method has been used to study heat transfer in two phase micro channel flows by Silvério and Moreira (26).

All the instrumentation is triggered by the same signal, emitted as the drop crosses a horizontal laser beam aligned with a photodiode.

Characterization of the substrates

Smooth surfaces of different materials, namely stainless steel AISI316 and aluminum were used to validate the model for different wall effusivities, ε_w, of $7.2 \cdot 10^3 kg/Ks^{2.5}$ and $14 \cdot 10^3 kg/Ks^{2.5}$, respectively.

Each pair liquid-surface is characterized by the equilibrium contact angle, θ and by the surface topography. For water drops, θ_1=93.0º and θ_1=93.5º for the stainless steel surface and θ_3=72.3º for the aluminum substrate (these values of θ were obtained at room temperature). Regarding the smooth glass surface ($R_a \approx 0\mu m$) used for visualization purposes, the contact angle with water is θ_2=38.5º. Complete wetting ($\theta \approx 0º$) is observed for all the surfaces when wetted by the ethanol and by the HFE7100 drops.

The topography is characterized by the roughness amplitude (mean roughness, R_a, determined according to standard BS 1134 and mean peak-to-valley roughness, R_z, calculated according to standard DIN4768). A summary of the main topographical characteristics of the targets used in this study is provided in Table 3.

A detailed description of the measurement procedures is presented in Moita and Moreira (27).

Table 3: Main topographical characteristics of the surfaces.

Surface	R_a [μm±10%]	R_z [μm]
Stainless steel	0.311	2.32
Stainless steel	0.524	9.0
Aluminum	1.5	14.1

RESULTS AND DISCUSSION

The current section presents the experimental results and discusses the theory behind the observed phenomena. It is divided in three main sub-sections: the first addresses the qualitative and quantitative description of the thermal and fluid dynamic behaviour of the liquid drops impacting onto a heated solid substrate, in the absence of liquid phase change. Main emphasis is placed in the discussion of the relative importance of the parameters influencing drop behaviour. The second sub-section introduces the theory used to describe the flow and temperature fields in the spreading drop. The theory allows estimating the contact temperature based on an analytical expression, function of the thermal effusivities of the liquid and of the substrate, weighted by the Prandtl number, to include the flow effects related to the thermal and hydrodynamic boundary layers developed during the spreading of the lamella. The theoretical estimations are then analysed, based on the comparison with the experimental results in the last sub-section.

Hydrodynamic and thermal behaviour of the impinging drops: influencing parameters

The dynamic behaviour of a drop impacting onto a solid and heated substrate is well known to depend on the heat transfer regime. In the absence of phase transition, the drop deforms and develops from the shape of a truncated sphere into that of a circular lamella surrounded by a thick rim, in an elongational flow around a stagnation point. Fig. 1 illustrates this process for HFE7100 and water drops impinging on a stainless steel substrate, recorded by the synchronized two high-speed cameras for both side and bottom views of the drop.

Given the low effusivity of the glass and the fact that for these surfaces the thermocouple could not be embedded in the centre of the impact region (beneath the drop), the contact

temperature as defined in (6) was used for comparative purposes.

At contact temperatures close to the boiling temperature of the liquid $T_c = 59$ºC, the side view of the drops shows a regular spreading behaviour without any thermal induced atomization. On the other hand, from the bottom view of the images it is evident a ring of bubbles around the stagnation point (e.g. at t=1.0ms in Fig.1a) which, given the low surface temperature, cannot be attributed to thermal effects. Instead, this ring is generated by a rarefaction wave within the impacting drop, which results from the reflection of the primary compression wave at the free surface of the drop (e.g. Chaves et al. [28]).

This set of images also evidences a few morphological features resulting from the significantly different thermo-physical properties of both liquids. Hence, there is no recoiling phase for the HFE7100 drop, so the lamella spreads for very long periods, clearly dominated by capillary forces, in a behaviour which is characteristic of complete wetting systems,

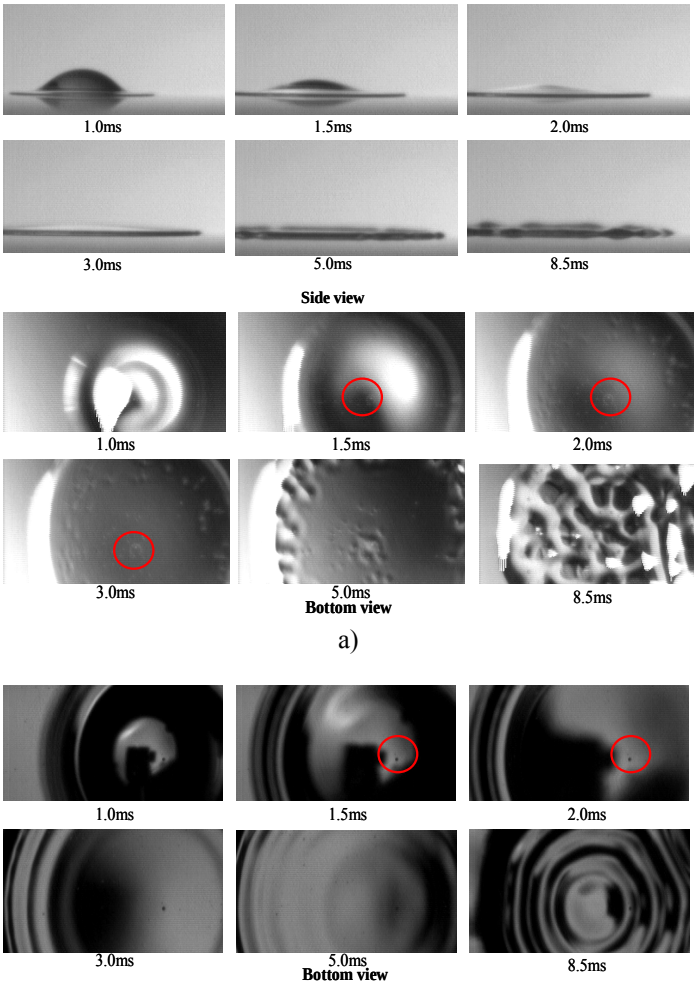

Figure 1: Details of the spreading of: a) a HFE7100 drop (D_0=2.0 mm, u_0=1.3 ms^{-1}, T_c=59ºC and b) a water drop (D_0=2.8 mm, u_0=1.3 ms^{-1}, T_c=90ºC) impacting onto heated transparent substrates. $\Delta T = T_{sat} - T_c$ is equivalent for both liquids.

for small or moderate impact velocities. Looking at the bottom views it is clear, from the image contrast, that the liquid flows from the central region to the periphery, which becomes thicker as the peripherical rim is formed at later stages of the spreading. Wavy disturbances are observed to start at $t > 4$ ms at the thin peripheral region of the lamella close to the rim, which remains weakly disturbed, and later around the stagnation region, at $t = 4.5$ ms.

A cellular structure becomes visible at the core region surrounded by the rim, (e.g. at $t = 8.5$ ms) in agreement with the observations reported by Chandra and Avedisian (29). This structure is attributed to surface tension gradients, due to non-uniform heat transfer during the spreading process and is more evident for the HFE7100 drop for which the σ_{lv} is 5times smaller than that of water and decreases with temperature at a larger slope.

This is consistent with the results shown in Fig. 2, which depicts the evolution of the instantaneous substrate temperature, for the impact of HFE7100 and water drops onto a stainless steel surface, at initial substrate temperatures equivalent to those depicted in Fig. 1. The plot depicts very late times after impact to give an overall perspective of the temperature evolution within the whole contact process. However, the most relevant processes occur very early after impact (at $t^* - t^*_0 < 5$, being t^*_0 the instant when the droplet contacts the surface and the temperature starts to decrease.

Since the liquid-drop interface temperature is below the saturation temperature of the liquid there is no phase transition. Nevertheless, the substrate temperature decreases suddenly, at droplet contact, given the fast heat transfer to the liquid, which is initially at room temperature. The larger specific heat of the water contributes significantly to decrease the surface temperature and promotes favourable conditions for rewetting. The effect of surface tension in the modification of the morphology of the spreading lamella, as discussed in the

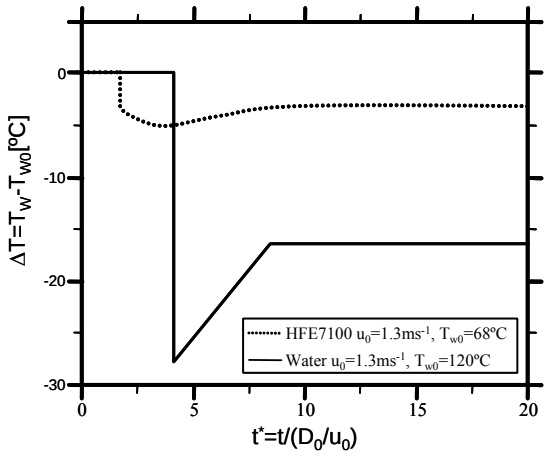

Figure 2: Instantaneous surface temperature, measured at the point of impact of HFE7100 (D_0=2.0 mm, u_0=1.3 ms^{-1}) and water (D_0=2.8 mm, u_0=1.3 ms^{-1}) drops colliding with a smooth stainless steel surface (R_a=0.311 μm, R_z=2.32 μm), without phase transition.

previous paragraph, further contributes to the overall smaller decay of the substrate temperature as it is wetted by the HFE7100 drop. Indeed, the occurrence of cellular structures further contributes to the non-uniform heating of the liquid film and to the promotion of its disruption and faster evaporation, thus decreasing the mass and contact time of the lamella over the surface. A similar trend was observed for the ethanol drops, for which σ_{lv} also decreases more with temperature when compared to water (e.g. Frohn and Roth [30]).

The effect of the impact conditions and particularly of the impact velocity is far less important, as demonstrated in Fig. 3, which illustrates the temporal variation of the substrate temperature during the collision of water and ethanol drops colliding at various velocities. Again, the larger heat capacity of the water leads to a higher drop of the substrate temperature.

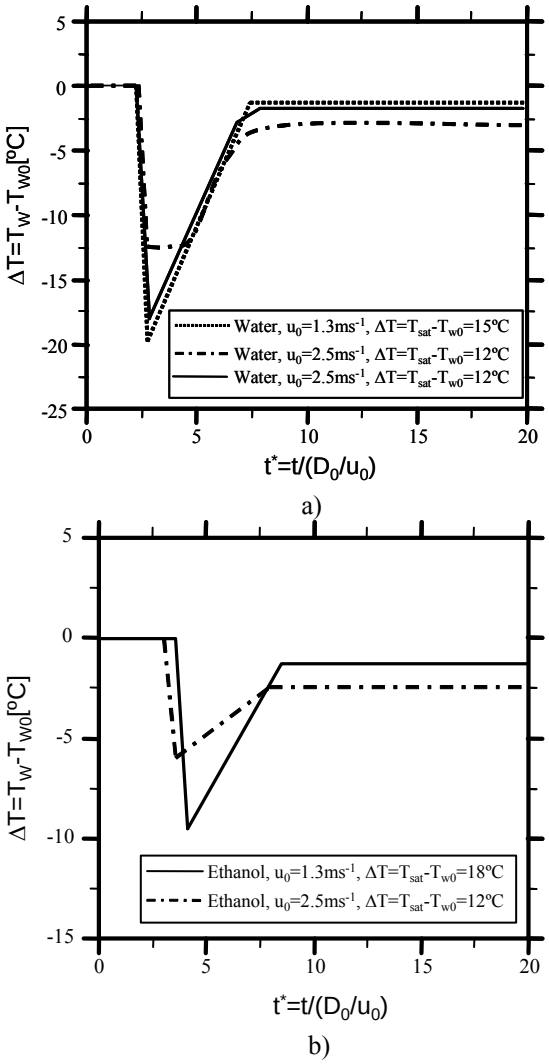

Figure 3: Instantaneous surface temperature, measured at the point of impact of: a) water (D_0=2.8mm) and b) ethanol (D_0=2.4mm) drops colliding with a smooth stainless steel surface (R_a=0.311μm, R_z=2.32μm), at different velocities. $\Delta T=T_{sat}-T_{w0}$=15ºC.

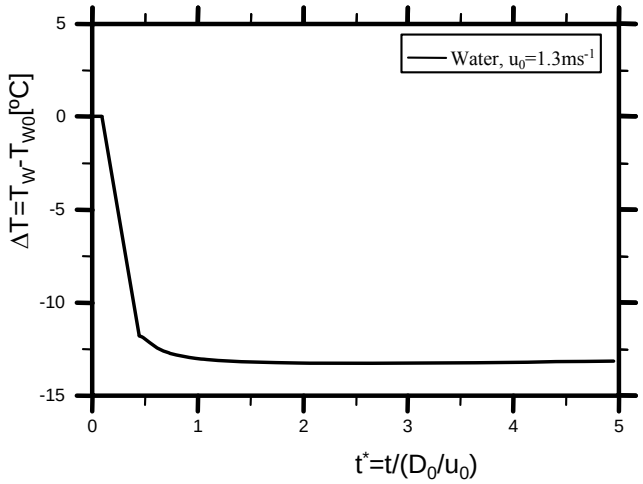

Figure 4: Variation of the instantaneous temperature within the earlier instants after impact of a water drop (D_0=2.8mm) on a smooth stainless steel surface (R_a=0.311μm, R_z=2.32μm). $\Delta T=T_{sat}-T_{w0}$=15ºC.

Given that the most relevant temperature variations occur within the earlier instants after impact, as illustrated in Fig. 4 for the impact of water drops, this is the important phase to be evaluated and modelled in terms of heat transfer phenomena.

The accurate evaluation of the phenomena described so far depends on the rate of heat exchange between the drop and the target which is determined by the contact temperature. The "conventional" contact temperature is determined as proposed by Seki and Sanokawa (6), from the solution available for two-semi-infinite solid, which mainly relates the contact temperature with the liquid and substrate temperatures weighted by the respective effusvities. However, regarding the spreading behaviour of the impinging drop, it is expected that the liquid flow would influence the value of the temperature at liquid-surface contact interface. In this context, an alternative expression is now proposed for the determination of the contact temperature, according to the formulation summarized in the following paragraphs.

Flow and the temperature fields in the spreading drop: Theory

When a drop impacts on a solid substrate it generates a radially spreading flow in the lamella. If the impact Reynolds and Weber numbers are high, the velocity field far from the wall can be described well by the remote asymptotic solution (31):

$$u_{r0}=\frac{r}{t+\tau}, \qquad u_{z0}=-\frac{2z}{t+\tau}+Z(t) \tag{1}$$

The constant τ is determined by the initial conditions. It is usually small (32) and can be neglected for large times after impact.

The flow field in an incompressible spreading drop with constant thermodynamic properties satisfies the full Navier-Stokes equations and no-slip conditions at the wall surface, as obtained in (33) in the form:

$$u_r = \frac{r}{t} g'(\xi), \qquad u_z = -2g(\xi)\frac{\sqrt{\nu}}{\sqrt{t}}, \tag{2}$$

where the self similar coordinate ξ is defined by:

$$\xi = \frac{z}{\sqrt{\nu t}} \tag{3}$$

and the scaled stream function $g(\xi)$ is the solution of the ordinary differential equation:

$$g'''+2gg''+\frac{1}{2}\xi g''+g'-g'^2 = 0 \tag{4}$$

which has to be integrated subjected to the no-slip boundary conditions at the wall and the condition of the flow approaching to the remote solution (1):

$$g = 0, \quad g' = 0 \quad \text{at} \quad \xi = 0, \tag{5a}$$

$$g' = 1 \quad \text{at} \quad \xi \to \infty. \tag{5b}$$

The energy equation:

$$\rho c_v \left(\frac{\partial T}{\partial t} + \mathbf{u} \bullet \nabla T \right) = \nabla \bullet \left(k \nabla T \right), \tag{6}$$

can also be written in the scaled form using the variable ξ:

$$2T'' + \mathrm{Pr}(\xi + 4g)T' = 0. \tag{7}$$

Equation (7) is valid also for the solid wall region with $g_{wall} = 0$.

A general form for the temperature distribution in the drop, T_d and in the wall, T_w is:

$$T_d = T_c + (T_{d0} - T_c)\frac{I_0(\mathrm{Pr}_d, \xi)}{I_0(\mathrm{Pr}_d, \infty)} \tag{8a}$$

$$T_w = T_{w0} + (T_c - T_{w0})\mathrm{erfc}\left[-\sqrt{\mathrm{Pr}_w}\frac{\xi}{2} \right] \tag{8b}$$

where:

$$I_0 = \frac{\sqrt{\mathrm{Pr}}}{\sqrt{\pi}} \int_0^{\xi} \exp\left[-\frac{\mathrm{Pr}}{4}\chi^2 - 2\,\mathrm{Pr}\int_0^{\chi} g(\zeta)d\zeta \right] d\chi \tag{9}$$

The temperature field (8) satisfies the boundary conditions:

$$T = T_{d0} \quad \text{at} \quad \xi \to \infty \tag{10a}$$

$$T = T_{w0} \quad \text{at} \quad \xi \to -\infty \tag{10b}$$

$$T_d = T_w = T_c \quad \text{at} \quad \xi = 0 \tag{10c}$$

where T_c is the unknown contact temperature. It is determined from the condition of continuity of the heat flux at the drop/wall interface $\xi = 0$:

$$k_d T_d' = k_w T_w' \quad \text{at} \quad \xi = 0 \tag{11}$$

Conditions (11) with the help of (8)-(9) yield the following expression for T_c:

$$T_c = \frac{\varepsilon_d T_{d0} + \varepsilon_w I_0(\mathrm{Pr}_d, \infty) T_{w0}}{\varepsilon_d + \varepsilon_w I_0(\mathrm{Pr}_d, \infty)} \tag{12}$$

Equation (12) is similar to the well-known expression for the temperature at the contact of two solid bodies.

Function $I_0(\mathrm{Pr}_d, \infty)$ can be obtained by numerical integration of (9) with the help of the numerical solution of (4). At very small Prandtl numbers (typical for liquid metals) the asymptotic solution is obtained in (34) in the form:

$$I_0(\mathrm{Pr}_d, \infty) \approx 0.447 + 0.271\sqrt{\mathrm{Pr}_d} \quad \text{at} \quad \mathrm{Pr}_d << 1 \tag{13}$$

At high values of the Prandtl number, the thermal boundary layer is much smaller than the thickness of the viscous boundary layer. Therefore, the function $g(\xi)$ can be linearized near the wall: $g(\xi) \approx g''(0)\xi^2/2$. In this case the integral in the right-hand side of (9) can be evaluated yielding:

$$I_0(\mathrm{Pr}_d, \infty) \approx e^{-y}\frac{9\sqrt{y}}{\sqrt{6\pi}}\left\{ \sqrt{12}\pi\left(I_{-1/3}y + I_{1/3}y \right) - 9e^{-y}\,\mathrm{pFg}\left[\begin{matrix} 1/2 & 1 \\ 2/3 & 4/3 \end{matrix}; -2y \right] \right\}, \tag{14}$$

where:

$$y = \frac{\mathrm{Pr}}{96\, g''(0)^2} \tag{15}$$

I is the Bessel function and pFg is the generalized hypergeometric function. The value $g''(0) \approx 1.0354$ is obtained from the numerical integration of (4).

As shown in Fig. 5, both inner and outer asymptotics describe well the function $I_0(\mathrm{Pr}_d, \infty)$ in the related regions. The value of this function in the region $\mathrm{Pr} \in [0.1, 10]$ is between 0.5 and 0.7.

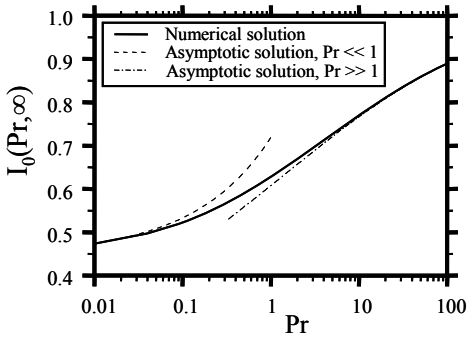

Figure 5: Comparison between the function $I_0(\mathrm{Pr}, \infty)$ and the asymptotics in eqs. (13) and (14).

Theoretical analysis: comparison with the experimental results

The theory predicts a constant value of the contact temperature in the phase when the thermal boundary layer is thinner than the thickness of the lamella (for $t^* \leq 2$), which is not entirely true, since there is a variation in the transient initial temperatures after impact. However, the average value for the correspondent time period is in quite good agreement with the predicted temperature. In this context, the theory may also explain the weak influence of the impact velocity in the variation of the substrate temperature at this period.

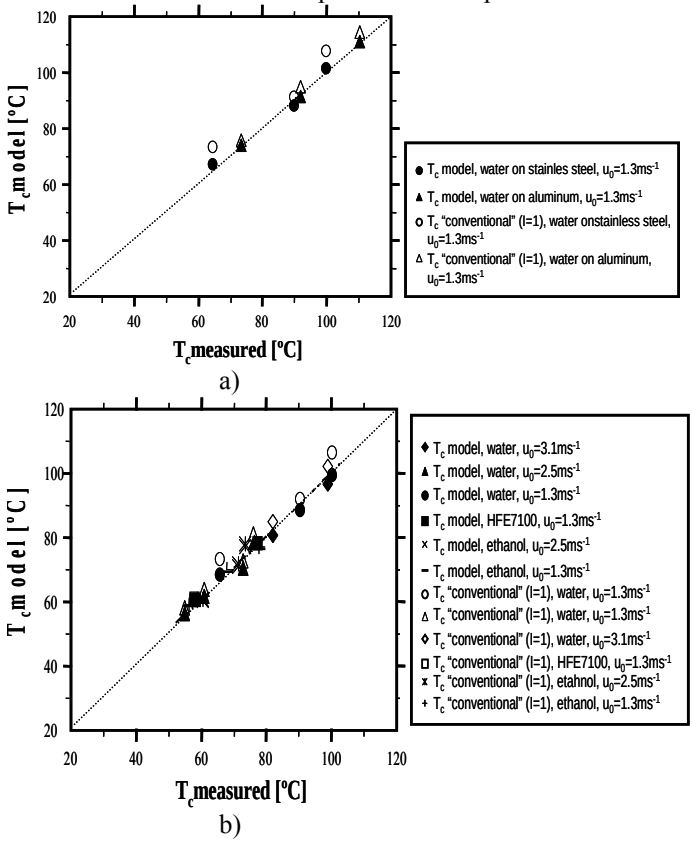

Figure 6: Comparison between the contact temperatures determined by the model proposed in the present paper and the expression suggested by Seki et al. (6), with the experimental results obtained for different impact conditions, for $t^* = t/(D_0/u_0 \approx 2)$. a) Effect of the substrate effusivity, for impacts onto smooth aluminum ($R_a = 1.5$ μm, $R_z = 14.1$ μm) and stainless steel ($R_a = 0.311$ μm, $R_z = 2.32$ μm) surfaces. b) Effect of liquid properties for impacts onto the smooth stainless steel substrate.

The surface effusivity has an important weight in the final value of T_c. For instance, for a similar $T_{w0} = 80$ºC, the contact temperature on the aluminium surface is about 5ºC larger than that obtained for the impact on the stainless steel surface, which is in agreement with the trend observed by Tartarini et al. (8). For much higher temperatures it is expected that this difference will increase. The experimental results are in good agreement with the proposed model being slightly better for the aluminum surface, when compared to the "conventional T_c" proposed in (6), probably because with such high surface effusivities, the relative effect of the flow in the final contact temperature becomes more important than when dealing with surface with low effusivities, which becomes probably the most important parameter. These trends are shown in the Fig. 6a).

When comparing the behaviour of droplets of different liquids, as depicted in Fig.6b), the agreement between the predicted T_c and the experimental data is rather good, despite the fact that no adjustable parameters are introduced in the model and it seems even better suited than the conventional expressional proposed in (6) for some conditions concerning the impact of water drops, for which the Prandtl number varies more with the temperature, thus highlighting the influence of the flow in the cooling performance. For the other liquids the Prandtl number is rather high so the difference between the T_c evaluated in the proposed model and the conventional T_c are is not so high. The effect of including the Prandtl number would be more evident for drops of liquid metals.

SUMMARY

This experimental and theoretical study is devoted to the investigation of non-isothermal impact of a single drop onto a semi-infinite solid substrate. Experimental observations show a strong change in the morphology of spreading drop at high initial wall temperatures, leading to bubbles entrapment, thermocapillary waves and cellular structure of the spreading flow. The evolution of the contact temperatures is measured in a wide range of the impact parameters, material and surface properties of the wall and liquid.

A theoretical model for the flow and temperature fields in the spreading drop leads to an explicit expression for the constant contact temperature. The agreement between the measurements and theoretical predictions of the contact temperature is rather good in a wide range of parameters.

ACKNOWLEDGMENTS

The authors acknowledge the contribution of the National Foundation of Science and Technology by supporting A.S.M. with a Fellowship (REF:SFRH/BPD/63788/2009) and by partially financing the research through the project PTDC/EME-MFE/69459/2006. I.R. acknowledges also the support of EU through the EXTICE project in the framework of FP7-AAT-2007-RTD-1. A.S.M. would also like to thank to Eng. Matteo Morais for his help in part of the measurements campaign.

REFERENCES

[1] Al-Ahmadi, H. M., Yao, S. C., 2008, "Spray Cooling of High Temperature Metals Using High Mass Industrial Nozzles", Exp. Heat Transf., **21**(1), pp. 38-54.

[2] Fest, S., Schmidt, J., 2009, "An Experimental Study of Intermittent Spray Cooling Above the Leidenfrost Point", Proc. ICLASS-2009, Vail, Colorado, USA.
[3] Van Dam, D. B., Le Clerc, C., 2004, "Experimental Study of the Impact of an Ink-jet Printed Droplet on a Solid Substrate", Phys. Fluids, **16**(9), pp. 3403-3414.
[4] Amon, C. H., Yao, S.-C., Hsieh, C.-C., 2005, "Microelectromechanical System-based Evaporative Thermal Management of Heat Flux Electronics", Trans. ASME, 127.
[5] Liu, J., Franco, W., Aguilar, G.., 2005, "The Effect of Roughness on the Impact Dynamics and Heat Transfer of Cryogen Droplets Impinging onto Indented Skin Phantoms", Proc. HT2005, San Francisco, CA, USA.
[6] Seki, M, Kawamura, H., Sanokawa, K., 1978, "Transient Temperature Profile of a Hot Wall Due to an Impinging Liquid Droplet", J. Heat Transf., **100**, pp. 167-169.
[7] Abu-Zaid, M., Atreya, A., 1989, "Effect of Water on Piloted Ignition of Cellulosic Materials", NIST Rept., GCR-89-561.
[8] Tartarini, P, Lorenzini, G., Randi M. R., 1999, "Experimental Study of Water Droplet Boiling on Hot, Non-porous Surfaces", Heat Mass Transf., **34**, pp. 437-447.
[9] Tartarini, P., Corticelli, M. A., Santangelo, P. E., 2009, "Droplet Cooling of Heated Surfaces: Experimental and Numerical Analysis", Proc. ICLASS-2009, Vail, Colorado, USA.
[10] Labeish, V. G.., 1994, "Thermodynamic Study of a Drop Impact Against a Heated Surface", Exp. Thermal Fluid Sci., **8**, pp. 181-184.
[11] Chen, J. C., Hsu, K. K., 1995, "Heat Transfer During Liquid Contact on Superheated Surfaces", J. Heat Transf., **117**, pp. 693–697.
[12] Pasandideh-Fard, M., Aziz, S. D., Chandra, S., Mostaghimi, J., 2001, "Cooling Effectiveness of a Water Drop Impinging on a Hot Surface", Int. J. Heat Fluid Flow, **22**, pp. 201-210.
[13] Di Marzo, M., Evans, D., 1987, "Dropwise Evaporative Cooling of High Thermal Conductivity Materials", Int. J. Heat Tech., **5**, pp. 126-136.
[14] Di Marzo, M., Evans, D., 1989, "Evaporation of a Water Droplet Deposited on a Hot Thermal Conductivity Surface", ASME J. Heat Transf., **111**, pp. 210-213.
[15] Di Marzo, M., Tartarini, P., Liao, Y., Evans, D., Baum, H., 1991, "Dropwise Evaporative Cooling", ASME HTD, **166**, pp. 51-58.
[16] Di Marzo, M., Tartarini, P., Liao, Y., Evans, D., Baum, H., 1993, "Evaporative Cooling Due to a Gently Deposited Droplet", Int. J. Heat Mass Transf., **36**(17), pp. 4133-4139.
[17] Chandra, S., di Marzo, Qiao, Y. M., Tartarini, P., 1996, "Effect of Liquid-solid Contact Angle on Droplet Evaporation", Fire Safety J., **27**, pp. 141-158.
[18] Healy, W. M., Hartley, J. G., Abel-Kalik, S. I., 2001, "On the Validity of the Adiabatic Spreading Assumption in Droplet Impact Cooling", Int. J. Heat Mass Transf., **44**, pp. 3869-3881.
[19] Turns, S. R., 1996, "An Introduction to Combustion: Concepts and Applications", Turns, S.R., McGraw-Hill.
[20] Özisik , M. N., 1985, "Heat Transfer: a Basic Approach", Mc-Graw Hill.
[21] Incropera, F. P., DeWitt, D. P., 1990, "Fundamentals of Heat and Mass Transfer", 3rd. Ed., John Wiley & Sons.
[22] Lemmon, E. W., McLinden, M. O., Huber, M. L., 2005, "NIST Standard Reference Database 12", US Secretary of Commerce.
[23] Moita, A. S., Moreira, A. L. N., 2008, "Boiling Morphology and Heat Removal of Impinging Coolant Droplets", Proc. ILASS 2008, Como Lake, Italy.
[24] Moita, A. S., Moreira, A. L. N., 2009, "Development of Empirical Correlations to Predict the Secondary Droplet Size of Impacting Droplets onto Heated Surfaces", Exp. Fluids, **47**, pp. 755-768.
[25] Nunes de Carvalho, C., Lavareda, G., Parreira, P., Amaral, A. Botelho do Rego, A. M., 2007, "Influence of Oxygen Partial Pressure on the Properties of Undoped InO_x Films Deposited at Room Temperature by rf-PERTE", J. Non-Crystalline Solids, **354**, pp.1643-1647.
[26] Silvério, V., Moreira, A. L. N., 2008, "Pressure Drop and Heat Convection in Single-phase Fully-developed, Laminar Flow in Micro Channels of Diverse Cross Section, Proc. 5th European Thermal-Science Conference, Eindhoven, The Netherlands.
[27] Moita, A. S., Moreira, A. L. N., 2007, "Drop Impacts onto Cold and Heated Rigid Surfaces: Morphological Comparisons, Disintegration Limits and Secondary Atomization", Int. J. Heat Fluid Flow, **28**, pp. 735-752.
[28] Chaves, H., Kubitzek, A. M., Obermeier, F., 1999, "Dynamic Processes Occurring During the Spreading of Thin Liquid Films Produced by Drop Impact on Hot Walls", Int. J. Heat Fluid Flow, **20**, pp. 470-476.
[29] Chandra, S., Avedisian, C. T., 1991, "On the Collision of a Droplet with a Solid Surface", Proc. R. Soc. London, Ser.A, **432**, pp. 13-41.
[30] Frohn, A., Roth, N., 2000, Dynamics of Droplets, Springer-Verlag Berlin, Heidelberg, Germany, pp. 6-8.
[31] Yarin, A. L., Weiss, D. A., 1995, "Impact of Drops on Solid Surfaces: Self-similar Capillary Waves and Splashing as a New Type of Kinematic Discontinuity", J. Fluid Mech., **283**, pp. 141-173.
[32] Roisman, I.V., Berberovic, E., Tropea, C., 2009, "Inertia Dominated Drop Collisions I: On the Universal Shape of the Lamella", Phys. Fluids, **21**,052103.
[33] Roisman, I.V., 2009, "Inertia Dominated Drop Collisions II: An Analytical Solution of the Navier-Stokes Equations for a Spreading Viscous Film ", Phys. Fluids, **21**,052104.
[34] Roisman, I.V., 2009, "Fast Forced Film Spreading on a Substrate: Flow, Heat Transfer and Phase Transition", J. Fluid Mech., accepted.

